

2

MRDC41082.16FR

Copy No. \_\_\_\_\_

MRDC41082.16FR

AD-A166 779

# INVESTIGATION OF FAST REACTION SAW ACCELEROMETER

FINAL TECHNICAL REPORT FOR THE PERIOD  
October 2, 1980 through September 30, 1984

DARPA ORDER NO. 4061  
CONTRACT NO. MDA903-81-C-0081

Prepared for

Defense Supply Service  
Department of the Army  
Washington, D.C. 20310

M.E. Motamedi  
805/373-4479

DTIC  
SELECTED  
APR 09 1986  
S D

Approved for public release; distribution unlimited

Sponsored by

Defense Advanced Research Projects Agency (DoD)  
DARPA Order No. 4061  
Under Contract No. MDA903-81-C-0081 issued by  
Department of Army, Defense Supply Service-Washington,  
Washington, D.C. 20310

"Contract effective dates from October 17, 1980 through September 30, 1984".

The views and conclusions contained in this document are those of the authors and should not be interpreted as necessarily the official policies, either expressed or implied, of the Defense Advanced Research Projects Agency or the U.S. Government.



Rockwell International

DTIC FILE COPY

86 4 9

006

UNCLASSIFIED

SECURITY CLASSIFICATION OF THIS PAGE

REPORT DOCUMENTATION PAGE

1a. REPORT SECURITY CLASSIFICATION <b>Unclassified</b>		1b. RESTRICTIVE MARKINGS	
2a. SECURITY CLASSIFICATION AUTHORITY		3. DISTRIBUTION/AVAILABILITY OF REPORT <b>Approved for public release; distribution unlimited.</b>	
2b. DECLASSIFICATION/DOWNGRADING SCHEDULE			
4. PERFORMING ORGANIZATION REPORT NUMBER(S) <b>MRDC41082.16FR</b>		5. MONITORING ORGANIZATION REPORT NUMBER(S) <b>MDA903-81-C-0081 DARPA Order No. 4061</b>	
6a. NAME OF PERFORMING ORGANIZATION <b>Rockwell International Microelectronics Research and Development Center</b>	6b. OFFICE SYMBOL <i>(If applicable)</i>	7a. NAME OF MONITORING ORGANIZATION <b>Director, Advanced Research Projects Agency</b>	
6c. ADDRESS (City, State and ZIP Code) <b>1049 Camino Dos Rios Thousand Oaks, CA 91360</b>		7b. ADDRESS (City, State and ZIP Code) <b>1400 Wilson Boulevard Arlington, VA 22209</b>	
8a. NAME OF FUNDING/SPONSORING ORGANIZATION <b>Defense Supply Service</b>	8b. OFFICE SYMBOL <i>(If applicable)</i>	9. PROCUREMENT INSTRUMENT IDENTIFICATION NUMBER <b>DARPA Order No. 4061</b>	
8c. ADDRESS (City, State and ZIP Code) <b>Department of the Army Washington, D.C. 20310</b>		10. SOURCE OF FUNDING NOS.	
		PROGRAM ELEMENT NO.	PROJECT NO.
		TASK NO.	WORK UNIT NO.
11. TITLE (Include Security Classification) <b>INVESTIGATION OF FAST REACTION SAW ACCELEROMETER (U)</b>			
12. PERSONAL AUTHOR(S) <b>Motamedi, M.E.</b>			
13a. TYPE OF REPORT <b>Final Technical Report</b>	13b. TIME COVERED FROM <b>10-02-80</b> TO <b>09-30-84</b>	14. DATE OF REPORT (Yr., Mo., Day) <b>NOVEMBER 1985</b>	15. PAGE COUNT <b>109</b>
16. SUPPLEMENTARY NOTATION <b>Approved for public release; distribution unlimited.</b>			
17. COSATI CODES		18. SUBJECT TERMS (Continue on reverse if necessary and identify by block number)	
FIELD	GROUP	SUB GR	
			<i>10 to the 10th year 0.0013</i>
19. ABSTRACT (Continue on reverse if necessary and identify by block number) <p>The objective is to develop SAW accelerometers with improved bias stability characteristics for moderately accurate inertial navigation. Methods of fabricating dual-resonator crystals with low absolute and differential aging characteristics have been developed. Tests have been performed at 10 Gs acceleration on integrated noise levels for simulated guidance system mission times of up to 20 min. Error rates less than 15 meters per hour in position of accuracy and velocity error less than 0.013 m/s have been achieved. Sensor device has a frequency stability of part in <math>10^{10}</math> with a dynamic range of <math>10^6</math>. Simulation shows a bit quantization of <math>1.3 \times 10^{-3}</math> m/s and frequency scale factor of 770 Hz/m/s<sup>2</sup> can be achieved. The concept of SAW accelerometer is based on construction of a SAW resonator on the surface of a piezoelectric quartz cantilever beam. Acceleration loading of the beam induces a surface strain in the resonator areas, resulting in a deviation of the center frequency. This frequency change is proportional to the acceleration input and it provides an inherent direct frequency digital output for the signal processing of the device.</p>			
20. DISTRIBUTION/AVAILABILITY OF ABSTRACT UNCLASSIFIED/UNLIMITED <input type="checkbox"/> SAME AS RPT. <input type="checkbox"/> DTIC USERS <input type="checkbox"/>		21. ABSTRACT SECURITY CLASSIFICATION	
22a. NAME OF RESPONSIBLE INDIVIDUAL		22b. TELEPHONE NUMBER <i>(Include Area Code)</i>	22c. OFFICE SYMBOL

(Block 19 Continued)

The investigation also includes beam design of the SAW accelerometers, SAW resonator and oscillator design, methods of device fabrication and techniques of device packaging. Some guidance system simulation and device application are presented. A complementary technique based on silicon sensor technology is also investigated for developing inertial devices which have advantages such as small size and low cost and can be used for fast reaction devices.

Accession For	
NTIS GRA&I	<input checked="" type="checkbox"/>
DTIC TAB	<input type="checkbox"/>
Unannounced	<input type="checkbox"/>
Justification	
By _____	
Distribution/	
Availability Codes	
Dist	Avail and/or Special



## TABLE OF CONTENTS

	<u>Page</u>
1.0 SUMMARY.....	1
2.0 INTRODUCTION.....	2
3.0 PROGRAM GOAL.....	5
4.0 TECHNICAL BACKGROUND.....	6
4.1 SAW Accelerometer.....	6
4.2 Piezoelectric Technology.....	6
4.3 SAW Resonator.....	9
4.3.1 Resonator Structure.....	9
4.3.2 SAW Resonator Substrate.....	12
4.3.3 Frequency and Temperature Stability.....	12
4.3.4 SAW Oscillator Testing.....	13
5.0 TECHNICAL APPROACH.....	16
5.1 Cantilever Beam Design.....	16
5.2 Design of SAW Resonator.....	19
5.3 Silicon Accelerometer.....	24
5.3.1 Device Structure.....	24
5.4 Guidance System Simulation.....	28
6.0 RESULTS.....	32
6.1 Fabrication of SAW Resonator.....	32
6.2 Test Box Assembly.....	33
6.3 Dynamic Testing.....	35
7.0 FUTURE PLANS.....	40
8.0 REFERENCES.....	41
APPENDIX A. RESEARCH FACILITIES.....	42

## LIST OF FIGURES

	<u>Page</u>
Fig. 1 X-ray spectrum of a well-oriented ZnO film sputtered on quartz substrate.....	8
Fig. 2 Different cavity structure of SAW resonator.....	11
Fig. 3 A complete SAW oscillator circuit mounted inside a TO-8 package.....	15
Fig. 4 Design schematic of a SAW cantilever beam sensor.....	17
Fig. 5 Beam thickness as a function of beam length for proposed proof mass. Minimum natural frequency is 200 Hz.....	18
Fig. 6 Design tradeoff for SAW accelerometer with natural frequency at 200 Hz.....	20
Fig. 7 Superimposed boundary patterns of 350 MHz SAW resonator. The scales are in microns.....	21
Fig. 8 Equivalent circuits for SAW resonator: (a) model for one-port resonator; (b) model for two-port resonator.....	22
Fig. 9 Theoretical simulation of complex return loss of the resonator designed for the SAW accelerometer.....	23
Fig. 10 Typical Si sensor chips, including one mounted inside a TO-8 package.....	25
Fig. 11 A typical Si monolithic accelerometer sensor.....	26
Fig. 12 Detailed structure of a Si cantilever beam sensor: (a) cross section of beam; (b) scale-up cross section for clarity.....	27
Fig. 13 Layout perspective of a cantilever SAW sensor with electrical equivalent circuit.....	29
Fig. 14 Measured count output of a SAW dual crystal sensor vs time. Total time was approximately 18 min with a 2 s gate time. Also shown is the computed velocity from integrating once, as well as the displacement as a result of integrating the counter output twice.....	31

## LIST OF FIGURES

	<u>Page</u>
Fig. 15 A finished quartz substrate containing a dual-crystal SAW resonator.....	34
Fig. 16 A typical acceleration output of a SAW sensor with 7 mV/G scale factor. The response is detected with a spectrum analyzer tuned to 36.3 Hz bandwidth.....	37
Fig. 17 A typical cross-axis response of a SAW accelerometer sensor at 2000 Hz.....	38
Fig. 18 A typical true-axis response of a SAW accelerometer sensor at 2000 Hz.....	39
Fig. A.1 Censor SRA-100 automatic step-and-repeat mask aligner and exposure system.....	43
Fig. A.2 JADE step-and-repeat projection aligner for DSW and mask processing.....	44
Fig. A.3 HP-8510 network analyzer with HP9836 controller.....	45
Fig. A.4 CVD reactors.....	46
Fig. A.5 RF sputtering system.....	47
Fig. A.6 Unholtz-Dickie Model 351 dynamic shaker.....	48



MRDC41082.16FR

## 1.0 SUMMARY

Fast reaction accelerometer technology based on surface acoustic wave (SAW) sensors and planar cantilever beam structures have been studied. The ultimate reaction capabilities of these devices are investigated and compared with present available inertial sensors. Methods of fabricating dual-resonator crystals with low absolute and differential aging characteristics have been developed. Also, hybrid oscillator circuitry has been studied and preliminary results using dual-resonator sensing crystals showed excellent stability, typically less than  $1 \times 10^{-10}$  for a second average times. Tests have also been performed on integrated noise levels for simulated guidance system mission times of up to 20 min. Error rates less than 50 m/h in position of accuracy have been achieved. These data indicate that SAW accelerometers are considerably better than existing moderately accurate sensors which commonly have error rates of one nautical mile (equivalent to 1,852 m) per hour. A computer-aided and completely automated system was developed for SAW sensor characteristics and aging data for collecting meaningful data on both temperature and frequency stability. This system has a major contribution to collecting data for long-term stability. An RF package with 50  $\Omega$  transmission lines was designed and fabricated to vacuum-seal the entire oscillator and hybrid circuitry.

The concept of SAW accelerometers is based on construction of a SAW resonator on the surface of a piezoelectric quartz cantilever beam. Acceleration loading of the beam induces a surface strain in the resonator areas, resulting in a deviation of the center frequency. This frequency change is proportional to the acceleration input, and it provides an inherent direct frequency digital output for the signal processing of the device. The investigation also includes beam design of the SAW accelerometers, SAW resonator and oscillator design, method of device fabrication, and techniques of device packaging. Some guidance system simulation and device applications are also presented.

## 2.0 INTRODUCTION

The application of surface acoustic wave (SAW) sensors for navigation guidance is described in several previous reports.<sup>1-3</sup> The objective is to develop SAW accelerometers with good bias stability for moderately accurate inertial navigation. For application in future tactical systems, these accelerometers need to be less expensive, more reliable, and smaller than the floated gyroscopic accelerometers or electromagnetic force-rebalance accelerometers now in use.

Inertial sensors are used for navigation guidance and flight control in airborne systems such as cruise and MX missiles. The cruise missiles use the force-rebalance accelerometer in which the current waveforms for electromagnetic forcing of the proof mass are digitized as pulses. Such accelerometers have a long warm-up time and require precision electronics, machining and assembly; hence, the cost is high.

Many technological approaches for more reliable inertial sensors have been reported. Those which have received much attention are solid state accelerometer,<sup>1</sup> piezoresistive<sup>2</sup> and SAW accelerometers.<sup>3</sup> These approaches use a "proof mass" which is connected to the host vehicle and contains a stress sensor. The stress sensor measures the force applied to the proof mass, which is proportional to the sensed acceleration of the host vehicle. These are "open-loop" sensors, because the force is not applied by a precision servo loop as in the case of the gyroscopic and pendulous accelerometers.

Planar cantilever devices as a solid state open-loop accelerometer show promise for meeting all system requirements without bearings or points of wear. Using established solid state IC technology, a circuit containing strain-sensitive elements on a cantilever beam substrate can be made. Acceleration forces on this device will cause surface strains that are sensed and processed by the electronic circuit. This type of accelerometer has the potential of being inexpensive because it uses little power and can be made small and reliable.



MRDC41082.16FR

In this work, we are reporting the cantilever beam SAW accelerometer as a new approach for solving many existing problems dealing with the conventional accelerometers. An existing problem is the large temperature range requirement. Conventional accelerometers cannot perform as well as cantilever devices over large temperature variations. For example, floated devices depend on fluid bouyancy and viscosity. They cannot be adequately matched over a large range of temperatures. Similarly, electromagnetic and drag-cup devices depend on the magnetic properties of materials which cannot be adequately matched over large temperature ranges. Also, the thermal expansion of dissimilar materials causes stresses or strains that lead to mechanical instability in clamped assemblies with repeated temperature cycling.

SAW technology offers an approach for an inherently digital acceleration sensor with no precision electronics and machining assembly. This technology uses established planar photolithography for low-cost fabrication. The associated electronics contain only one active element (transistor). Simplicity makes this an attractive candidate for digital sensor applications in future missiles and manned and unmanned aircraft. The sensing principle is based on strain effect on moving resonant frequency of a highly stable SAW resonator.

The SAW resonator is a strain-to-frequency converter. It consists of an interdigital transducer between reflective gratings on a piezoelectric (quartz) substrate. A signal applied to the transducer launches Rayleigh waves along the surface of the substrate, which are coherently reflected by the gratings. A feedback electronic circuit maintains the cavity in resonance. This uses a single power source and generates an output signal at the resonator frequency. An additional buffer amplifier may be required for signal-level shifting to compatible logic levels.

Longitudinal strain applied to the resonator cavity will cause a proportional change in its resonant frequency. This provides a bit rate frequency output proportional to strain input and forms the basis of the simplest SAW cantilever beam accelerometer. Acceleration applied at the clamped end is

MRDC41082.16FR

transmitted to the proof mass at the free end through bending stress. The resulting surface strain along the SAW resonator causes a frequency shift which is proportional to the applied acceleration.

For moderately accurate inertial guidance systems, the integrated errors in accelerometers in positional accuracy are typically 1800 m/h. SAW-resonator accelerometers typically possess a dynamic range of  $1 \times 10^6$  and a full-scale frequency deviation of 200 ppm, corresponding to 10 Gs of acceleration. Recent studies involving the double integration of SAW accelerometers indicate a position accuracy of 50 m/h is achievable.



MRDC41082.16FR

### 3.0 PROGRAM GOAL

The goal of this program is to perform fundamental studies on SAW sensors using quartz substrates with improved bias stability characteristics. Methods of fabricating dual-resonator SAW sensors with low differential aging need to be developed. Dual-resonator crystals combined with hybrid oscillator circuitry has shown excellent achievable stability on the order of  $1 \times 10^{-10}$ . Solid-state sensors of this kind perform a position error smaller than 50 m/h mission time. A complementary technique based on Si monolithic technology will be investigated for developing inertial sensors. Devices of this kind demonstrate advantages such as small size, low cost and ease of signal processing.

## 4.0 TECHNICAL BACKGROUND

### 4.1 SAW Accelerometer

Accelerometers are needed for guidance, stability augmentation, and navigation of guided missiles and aircraft. For applications in future tactical systems, these accelerometers should be less expensive, more reliable, and smaller than the floated gyroscopic accelerometers, drag-cup velocity meters or electromagnetic force-rebalance accelerometers now in use. For missiles and other applications where rapid reaction is a necessity, these devices need to be able to operate without first being thermally stabilized at a given operating temperature.

One important task in this program is to perform studies on SAW temperature compensation methods that yield improved stability characteristics required of inertial navigation accelerometers. Also included in this program will be an evaluation of the transient thermal response of the SAW resonator cavity and amplifier electronics and the feasibility of meeting the program requirements.

Ideally, the acceleration sensor should be able to operate over the full operational range of ambient temperatures without temperature control. Depending on system applications, this temperature range can be as great as 179°C for Class IV avionics, or as small as 109°C for Class I avionics. Conventional accelerometers are not likely to perform as well as cantilever devices over such large temperature variations because their design depends on different properties of different materials, and these are difficult to maintain in the proper relationship over the large variations in temperature.

### 4.2 Piezoelectric Technology

SAW accelerometers require some kind of piezoelectric medium to be a part of sensor element. In the case of monolithic Si accelerometer, a ZnO film is used for piezoelectric material; while in the case of the SAW accelerometer, a substrate-like single crystal quartz acts as a piezoelectric medium. In this section, we will discuss each case in more detail.

MRDC41082.16FR

The Si monolithic accelerometer is a solid state sensor with a piezoelectric capacitor fabricated on the surface of a miniature cantilever beam. ZnO is a portion of a "sandwich" of materials which constructs the piezoelectric capacitor.

In our laboratory, we are using a Perkin Elmer RF sputtering unit modified for magnetron sputtering of ZnO. The system has a planar disc target of ZnO doped with  $\text{Li}_2\text{CO}_3$ . The substrate holder contains a substrate heater embedded inside a stainless steel cover, and the temperature is monitored throughout the process and is recorded on a strip chart recorder. Sputtering gaseous mixtures are carefully controlled in terms of composition, purity and pressure. Typically a mixture of argon-to-oxygen is used in the ratio of 80:20.

The primary nondestructive technique used to characterize the orientation and quality of these films is x-ray diffractometry. Using a Geiger counter with  $\text{Cu-K}\alpha$  radiation, the  $2\theta$  Bragg angle for either ZnO or Si is measured. Figure 1 shows an x-ray spectrum of the ZnO films on the fused quartz. This technique measures the distribution of crystal orientations in the polycrystalline films. The deposition conditions were optimized in this manner, and films with excellent orientation for the monolithic accelerometer were obtained.

The SAW accelerometer is also a solid-state sensor based on the property of SAW propagation. All SAW devices are based on some form of piezoelectric effect, which is necessary to transform an electrical signal at the input into a mechanical or acoustic signal. Traditionally, the substrate for a SAW device has been a large, single-crystal substrate using a piezoelectric insulator material. The crystal supplies both the piezoelectric effect needed and the substrate along which the surface acoustic wave signal propagates. The physics of SAW on such a substrate are complicated by the anisotropy of the material, but are otherwise straightforward. When SAW devices are constructed on the surface of a piezoelectric substrate, orientation and crystal growth of



MRDC41082.16FR

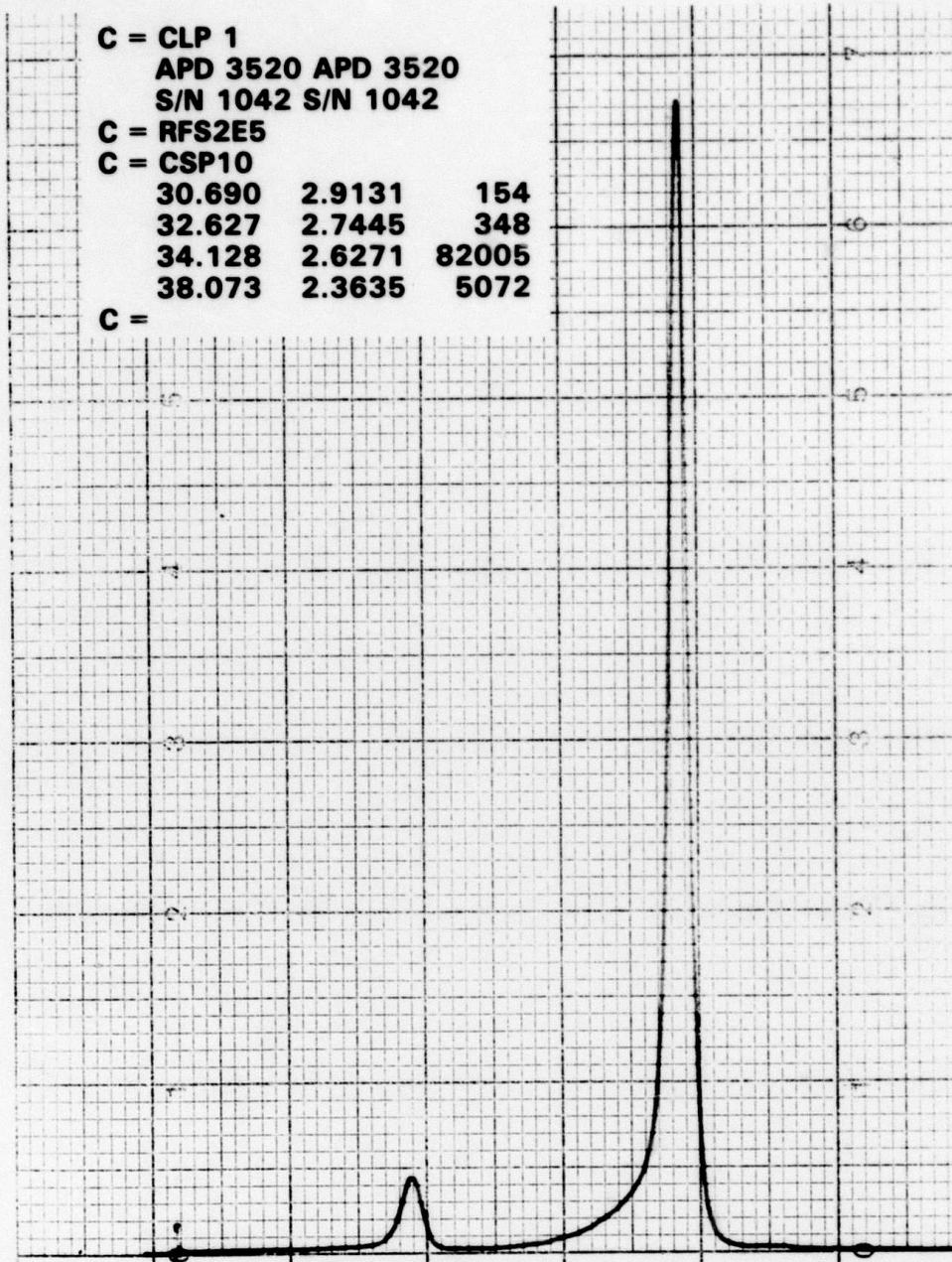


Fig. 1 X-ray spectrum of a well-oriented ZnO film sputtered on quartz substrate.

the substrate should be considered for characterization of the piezoelectric coupling and SAW propagation.

#### 4.3 SAW Resonator

The SAW resonator can be fabricated on the surface of the piezoelectric substrate, like quartz, using a planar process technology. This device can be used as a feedback element for precise, high-frequency oscillation. A SAW resonator consists of two reflectors and one or two interdigital transducers which together form a resonance cavity.

For the past ten years, SAW oscillators have been competing as alternative IF frequency sources to bulk wave crystal oscillators. They are currently used in numerous military and satellite applications, resulting in a power savings of 100:1 and a size reduction of 20:1 over bulk oscillators. SAW oscillators operate at fundamental frequencies beyond 1 GHz and have properties which effectively improve phase noise performance to the elimination of frequency multipliers and phase lock loop circuitry.

In controlling device characteristics such as temperature-compensated frequency stability, high-Q and low phase noise, the choice of substrate materials is an important decision in the design. To date, single-crystal quartz is used with several different crystal orientations applied. The lowest temperature coefficients have been achieved with the ST cut quartz. Since SAW resonators are presently fabricated on piezoelectric substrates, hybrid circuit technology must be used to construct a SAW oscillator.

##### 4.3.1 Resonator Structure

The SAW resonator is a planar electrode structure photolithographically defined on a suitable piezoelectric material. The SAW resonator functions in the same manner as a conventional quartz oscillator crystal. Acoustic waves are generated by an interdigital transducer which provides electrical-to-mechanical as well as mechanical-to-electrical signal transduction. The acoustic waves are confined within a cavity whose boundaries are accu-

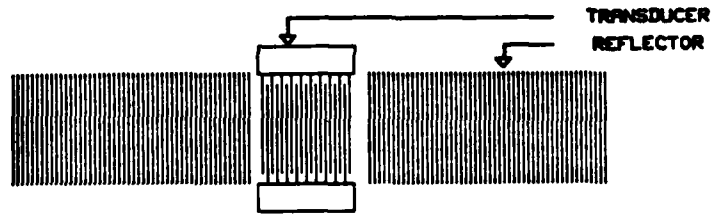
MRDC41082.16FR

rately maintained. The  $Q$  of the cavity is determined by the material losses and cavity leakage. The same excellent frequency controlled properties of bulk wave quartz resonators is also achieved by SAW resonators, provided the fabrication techniques are closely controlled. Figure 2 is a schematic representation of three common types of resonator designs. The simplest type is that shown in Fig. 2a, which is a single-pole, single-port resonator structure.

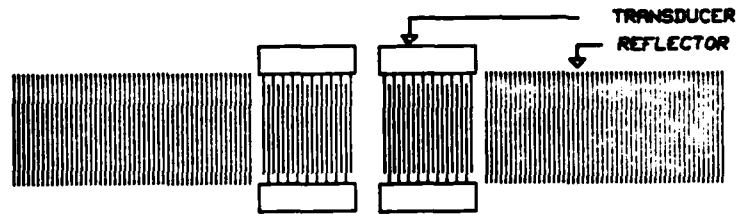
The single-pole, single-port resonator of Fig. 2a has inherently low crosstalk and lower insertion loss. The structure shown in Figs. 2b and 2c has a higher insertion loss due to propagation losses of an acoustic signal in the center of the cavity. However, these types of resonators have the advantage of existing in a  $180^\circ$  phase shift required for the construction of a positive feedback resonator controlled oscillator.

On either side of the input/output transducer are two gratings which contain a large number of reflecting structures with a periodicity slightly less than that in the transducer. The gratings act as mirrors when the acoustic wavelength is approximately equal to twice the grating periodicity. In this frequency range, all of the surface acoustic wave energy is confined within the cavity formed by the two gratings. Each grating acts like a mismatched impedance in the transmission line, causing a reflection. With a sufficient number of gratings, a total reflection from all the gratings can be achieved very nearly equal to the incident wave from the IDT transducer. At the resonance frequency, all of the reflections add in phase, resulting in a narrow-band signal with extremely high  $Q$  factor.

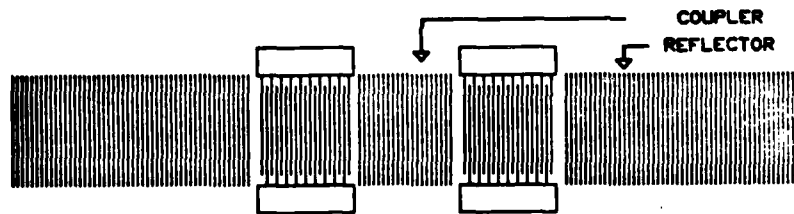
Although the single port resonator has many desirable properties, it does not have the design flexibility of the two-port device. When inserted in an oscillator circuit, the single-port resonator must be phase-shifted almost  $180^\circ$  to feed back an in-phase signal into the input of the amplifying active device in the oscillator. The two-pole device, on the other hand, allows for the  $180^\circ$  phase shift simply by reversing the connection leads in the second IDT structure, thus reversing the phase. Achieving the  $180^\circ$  required phase



SAW SINGLE PORT RESONATOR



SAW 1 POLE 2 PORT RESONATOR



SAW 2 POLE 2 PORT RESONATOR

Fig. 2 Different cavity structure of SAW resonator.



MRDC41082.16FR

shift in the single-port resonator may, in fact, increase the phase noise beyond what can be achieved by a conventional two-port resonator.

#### 4.3.2 SAW Resonator Substrate

Factors that influence substrate material selection include fractional bandwidth, insertion loss, temperature operating requirements and frequency stability vs temperature. While several piezoelectric materials have been used in SAW devices, their application characteristics differ significantly. Lithium niobate is a high coupling material used when wide fractional bandwidths are required where temperature coefficients up to 100 ppm/°C are acceptable. The insertion loss using quartz substrates for wide-band applications is usually unacceptable. For narrower band applications, quartz is most often used because of its increased stability capability. Quartz is also capable of providing total frequency shifts that are smaller than 30 ppm for a 0 to 60° commercial temperature range, and that are nominally less than 100 ppm in temperature-compensated oscillator circuits over the military temperature range of -55 to +85°C.

#### 4.3.3 Frequency and Temperature Stability

In its laboratories, Rockwell has developed temperature-compensating circuits which maintain the oscillator on a given frequency through a high accuracy over a wide temperature range. For example, a 324 MHz oscillator circuit was maintained within 30 ppm over the temperature range from 0 to 100°C by using temperature compensation circuitry. By minimizing the SAW drift with temperature compensation circuitry, a narrower bandwidth phase-locked loop can be tolerated when the SAW oscillator is operated with a subsystem or for application such as SAW sensors.

During years of experience in building SAW devices, Rockwell has conducted extensive aging tests in the 300 to 400 MHz region. Several factors concerning SAW aging characteristics have been determined. For example, to minimize aging, a hermetically sealed, vacuum-baked and vacuum-evacuated



MRDC41082.16FR

packaging approach must be used. In addition, die attached materials for positioning the SAW in the package must contain no materials which may outgas and deposit monolayers of organics or other materials onto the SAW cavity, thus affecting its operation over time and causing a shift in frequency and degrading the frequency stability data. All these studies and precautions in the laboratory have led to present frequency stability of better than one part in  $10^{10}$ .

The quantitative determination of resonator aging was a major task of a study conducted for stability. The amount by which a quartz resonator, bulk or SAW, changes with time is very small. Measurement accuracies of 0.1 ppm or less are required over time periods ranging up to one year. Because the resonator is a passive device, the conventional method is to build oscillator circuitry with the resonator as the frequency feedback element. Techniques like on-chip temperature compensation, dual-channel SAW resonator, and advanced high-vacuum sealing result in the state-of-the-art of both frequency and temperature stability.

#### 4.3.4 SAW Oscillator Testing

An automated testing system monitored the aging measurements. Software for the aging measurements was designed to control the system hardware and to take measurements periodically. This was accomplished using a real-time clock with battery back-up in conjunction with a Hewlett-Packard desktop computer. Using this system, resonator aging data were taken automatically. Extensive aging data were obtained using this automated test system. Resonators were interrogated periodically through the switches by a network analyzer, frequency synthesizer and counter, all of which were controlled by the desktop computer. Resonant frequencies were measured, oven temperatures were recorded, and time was logged from the computer's real-time clock. In this manner, the frequency/temperature drift was trapped with time. Software computed the differential drift between packaged pairs of SAW resonators.



MRDC41082.16FR

To minimize interaction from the other circuit components, we prefer that the SAW device be separately packaged in its own hermetically sealed enclosure. Figure 3 shows a typical impedance-matched SAW package which is connected to the remainder of the oscillator circuitry through impedance-matched microstrip lines.

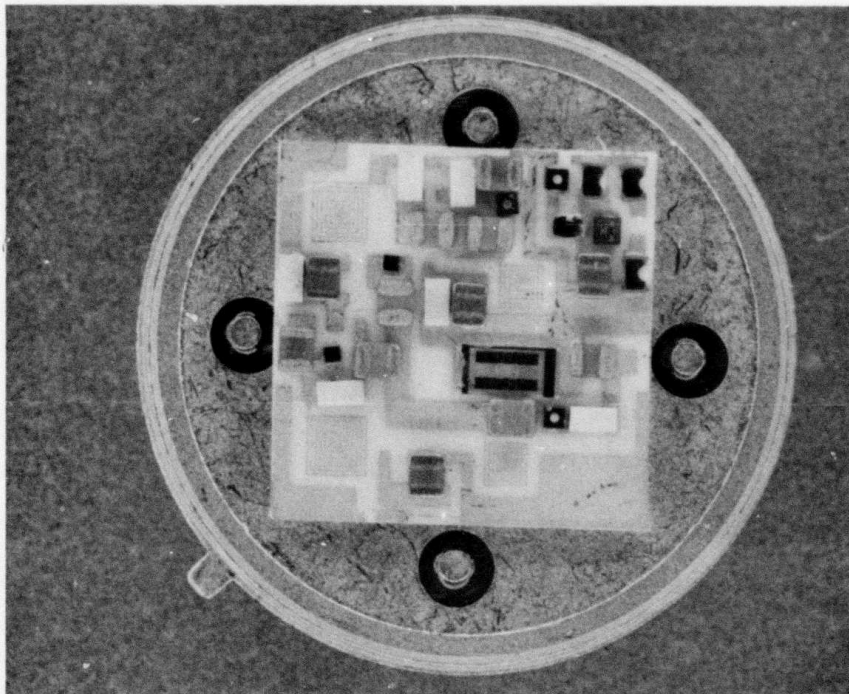


Fig. 3 A complete SAW oscillator circuit mounted inside a T0-8 package.

## 5.0 TECHNICAL APPROACH

5.1 Cantilever Beam Design

For preliminary design analysis, the objectives are to determine the important performance characteristics and design parameters, and to get a rough idea of their expected ranges. Thus, we consider just the simplified design shown in Fig. 4, which shows a simple, rectangular solid beam of length  $L$ , breadth  $b$  and height  $h$  clamped at one end. The free end is loaded by a proof mass of diameter  $d$ . The important performance characteristics of this device are the "detection threshold"  $a_d$  and the lowest natural resonant frequency  $f_n$ . Let us assume that the proof mass is made of invar, which has a density of  $8 \text{ g/cm}^3$ . Therefore, the proof mass will be:

$$m = 8\pi (d/2)^2 b \quad (1)$$

The natural resonant frequency of the beam will then be the following:

$$(2\pi f_n)^2 = \frac{bh^3 E}{4mL^3} \quad (2)$$

where  $E$  is Young's modulus for the beam material (quartz). Using Eqs. (1) and (2), the following formula for the diameter of the proof mass can be derived:

$$d = \frac{[Eh^3 / (8\pi L^3)]^{1/2}}{2\pi f_n} \quad (3)$$

Assuming a constant minimum natural frequency of 200 Hz, a family of curves of beam thickness as a function of beam length is shown in Fig. 5. In this plot, the diameter of the proof mass is chosen as a step variable.

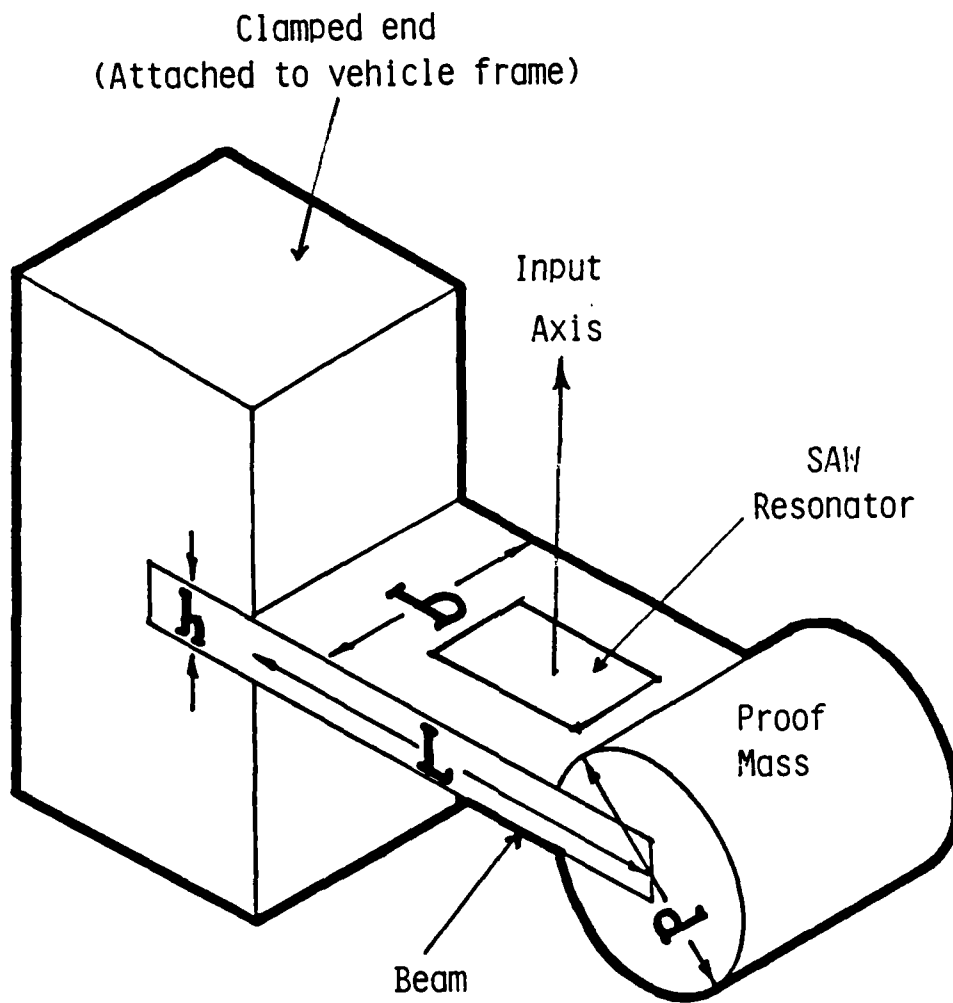


Fig. 4 Design schematic of a SAW cantilever beam sensor.

MRDC41082.16FR

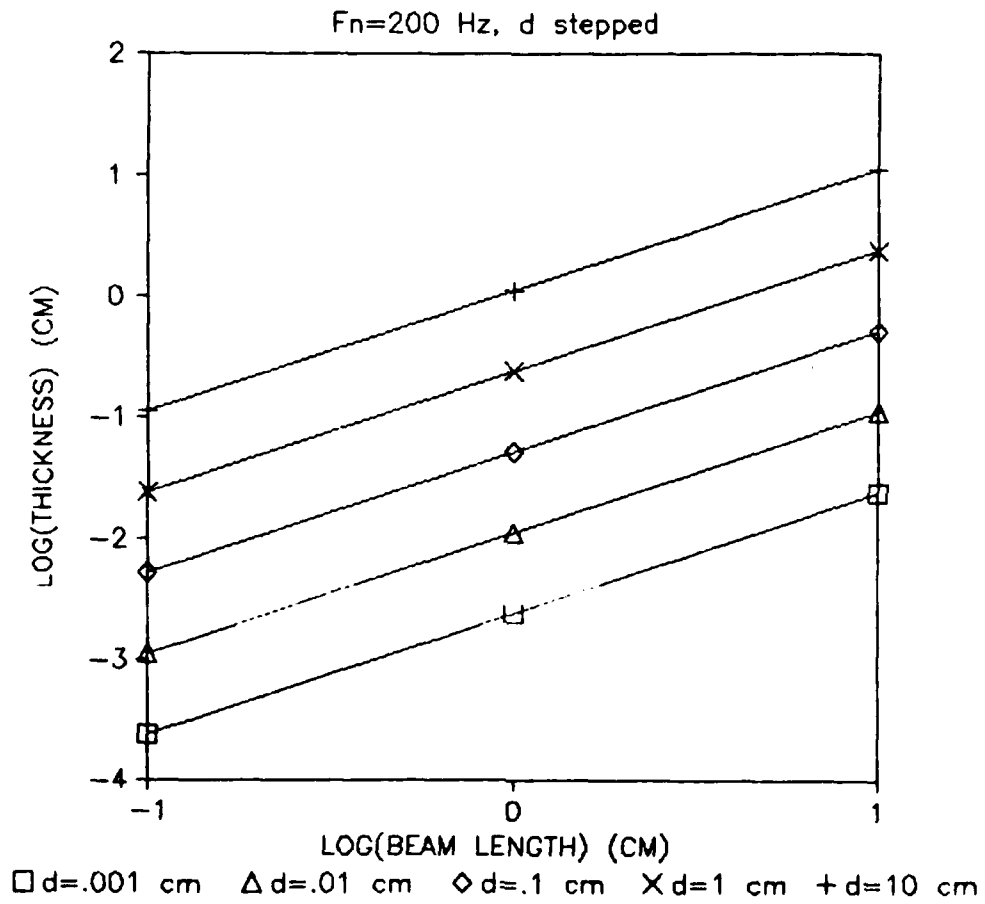


Fig. 5 Beam thickness as a function of beam length for proposed proof mass. Minimum natural frequency is 200 Hz.

MRDC41082.16FR

To derive a relation for minimum detectable acceleration of the beam as a function of the beam dimensions, we will consider our current frequency "noise floor" of  $10^{-10}$  stability. These data are already reported and correspond to a minimum detectable strain of about  $10^{-10}$  parts/part. The strain at the surface of the beam at the beam "root" is related to the acceleration by the following formula:

$$s = \frac{6Lma}{Ebh^2} \quad (4)$$

Combining Eqs. (1) to (4), the minimum detectable acceleration can be derived:

$$a_d = 10^{-10} \frac{2(2\pi fn)^2 L^2}{3h} \quad (5)$$

Assuming a constant minimum natural frequency of 200 Hz, a family of curves of beam thickness as a function of beam length shown in Fig. 6. In this plot, the minimum detectable acceleration  $a_d$  is chosen as a step variable in the unit of Gs.

## 5.2 Design of SAW Resonators

A SAW resonator is the actual sensor in SAW accelerometer. A set of the masks has been designed for the SAW resonator at 350 MHz range. Figure 7 shows the superimposed boundary patterns of the three masks required for the resonator. The resonator device has a size of 4 x 7 mm and a line resolution of 2  $\mu$ m.

To simulate a substrate resonator, an equivalent circuit like the one shown in Fig. 8 is used. Elements of both circuits are quite similar, with  $C_r$ ,  $L_r$  and  $R_r$  as resonant elements.  $C_0$  is the static capacitance of the IDT where  $R_s$  and  $L_s$  are the parasitic resistance and parasitic conductances, respectively. Using the equivalent circuit model, the amplitude and phase response of the designed resonator are shown in Fig. 9.

MRDC41082.16FR

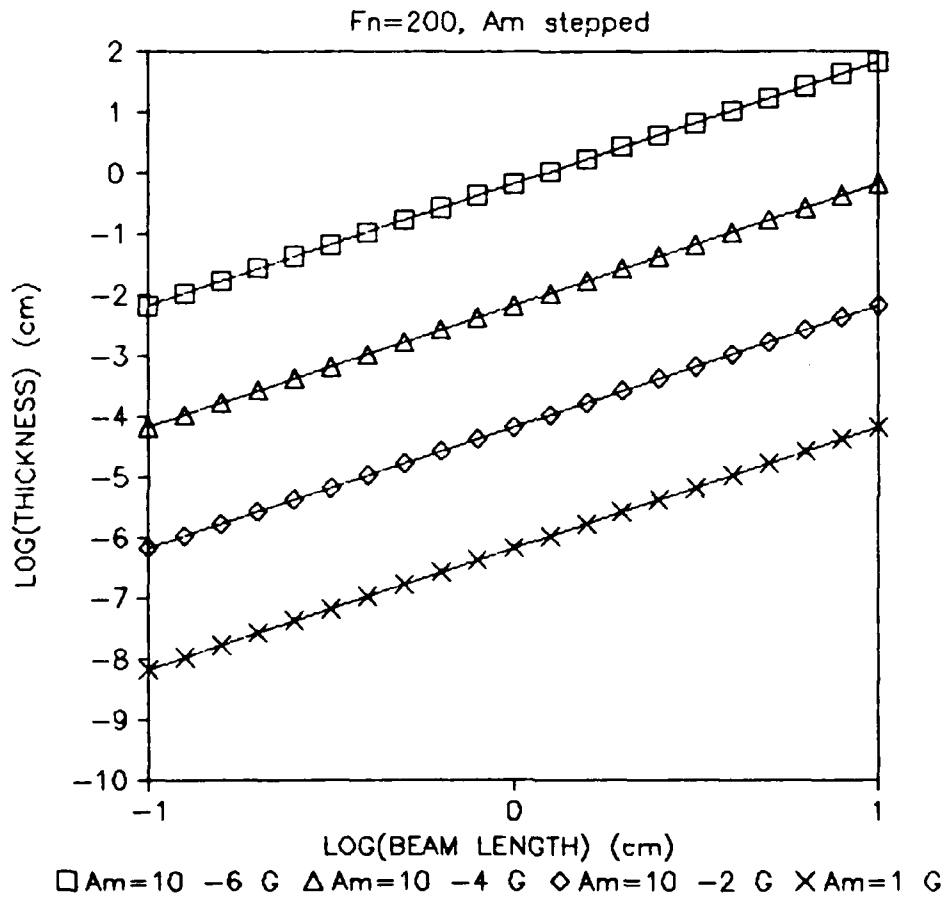


Fig. 6 Design tradeoff for SAW accelerometer with natural frequency at 200 Hz.

MRDC41082.16FR

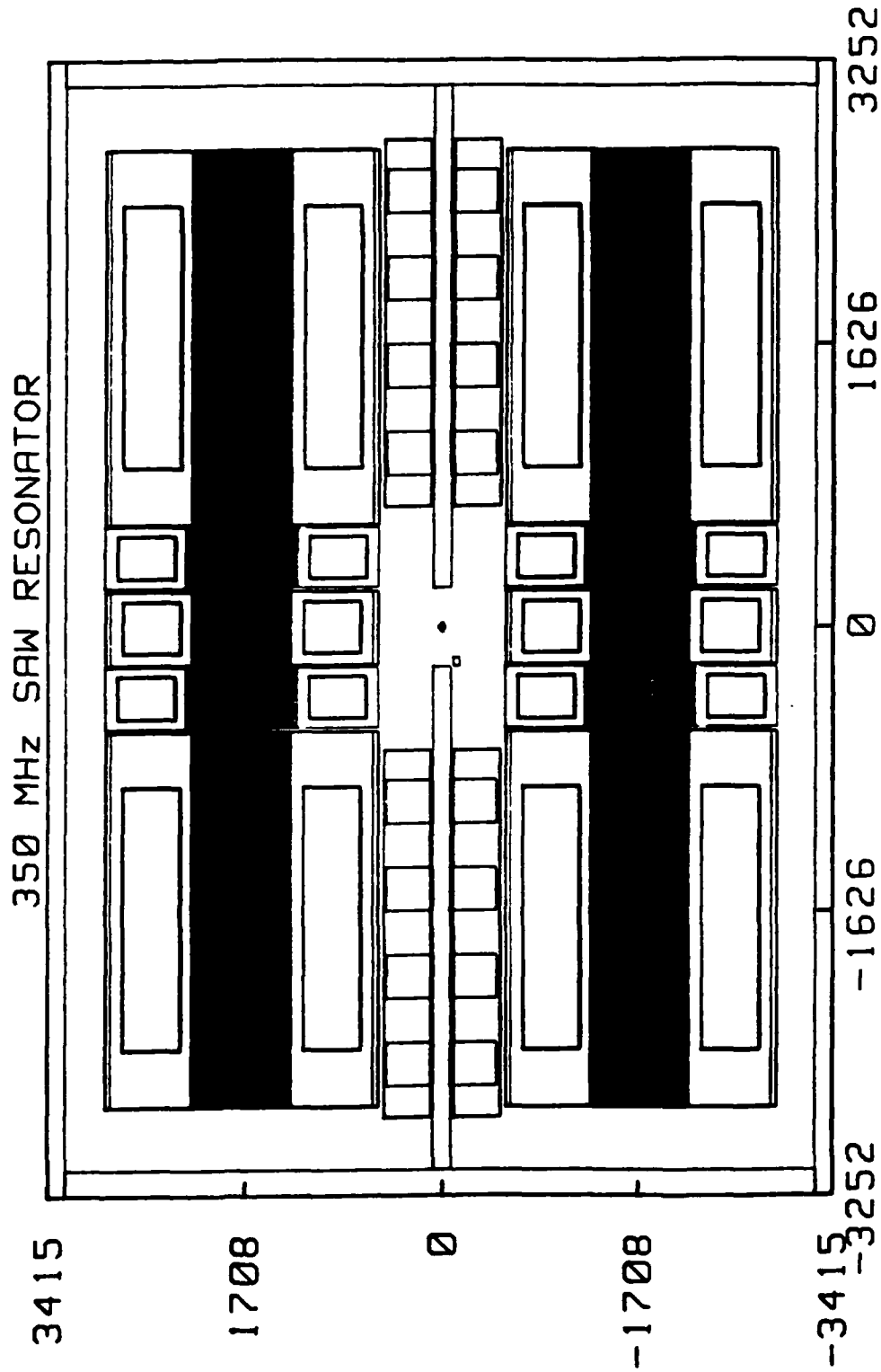


Fig. 7 Superimposed boundary patterns of 350 MHz SAW resonator. The scales are in microns.

MRDC41082.16FR

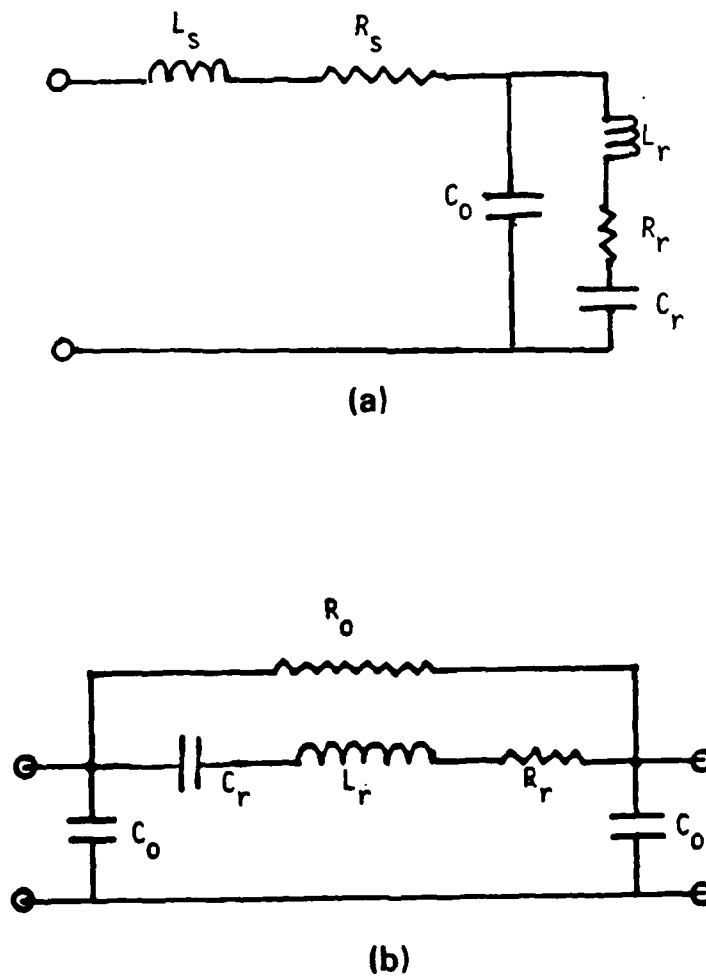


Fig. 8 Equivalent circuits for SAW resonator: (a) model for one-port resonator; (b) model for two-port resonator.

MRDC41082.16FR

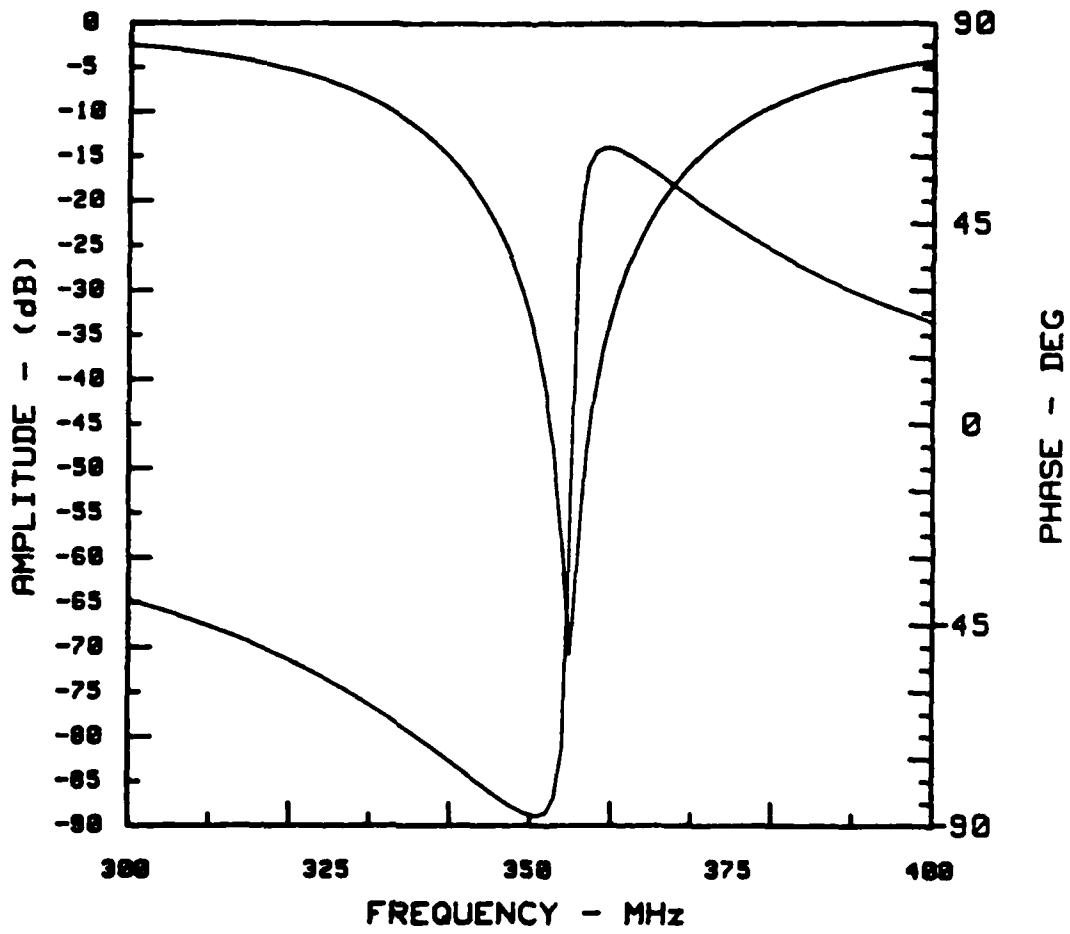


Fig. 9 Theoretical simulation of complex return loss of the resonator designed for the SAW accelerometer.

### 5.3 Silicon Accelerometer

Figure 10 is a photograph of typical Si accelerometer chips, where one chip is mounted inside a TO-8 package with wire bonds to the device contacts. Shown in Fig. 11 is a more detailed microphotograph of the chip. The monolithic accelerometer is an IC containing an acceleration sensor. The acceleration sensor consists of a miniature cantilever beam containing a thin-film piezoelectric capacitor on top. This beam is etched out of a part of the Si "chip" using advanced etching techniques. Acceleration forces normal to the surface of the chip cause the beam to bend, and this induces strain in the piezoelectric capacitor. The piezoelectric effect converts this strain into an electrical charge which is proportional to the acceleration. The charge is stored in the capacitor, so that the electrical potential at the output of the capacitor is again proportional to acceleration. The electrical signal is buffered by an on-chip PMOS transistor, which prevents the charge from leaking to ground. The on-chip IC also includes a temperature-compensating capacitor to cancel pyroelectric effects.

The monolithic accelerometer has the essential military requirements of small size, low weight and low power consumption. It uses the low-cost photolithographic fabrication methods developed for the IC industry.

#### 5.3.1 Device Structure

Figure 12 shows two cross sections of the cantilever beam with its integrated piezoelectric thin film capacitor. In Fig. 12b, the apparent thicknesses of the layers have been scaled up to provide visibility.

The piezoelectric capacitor consists of a "sandwich" of materials. The outside of the sandwich consists of two conducting layers. The bottom conductor is formed in the Si substrate by implantation of ions through a thin ( $0.1 \mu\text{m}$ ) layer of  $\text{SiO}_2$ . The top conducting layer is Al. The center of the sandwich is a film of  $\text{ZnO}$ , deposited by sputtering. An important attribute of this film is its piezoelectric property. This is fundamentally a material property, in which strain of the material causes an internal migration of

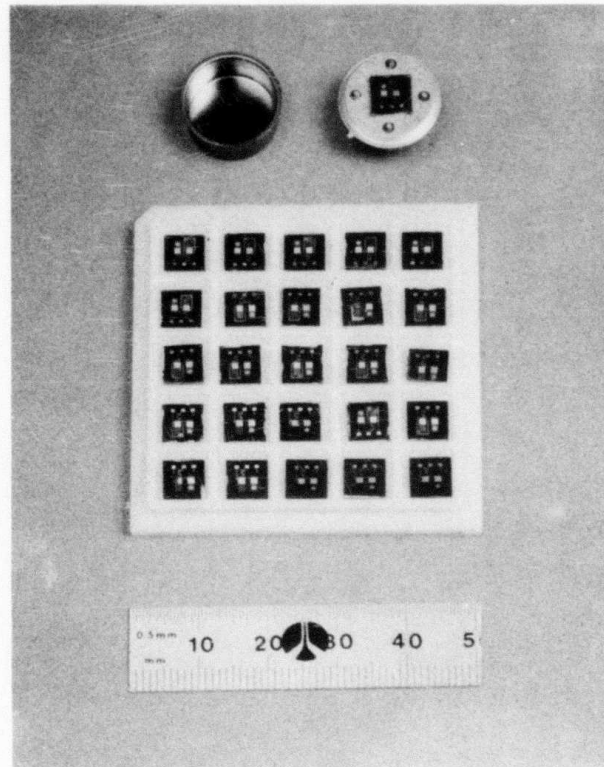


Fig. 10 Typical Si sensor chips, including one mounted inside a T0-8 package.

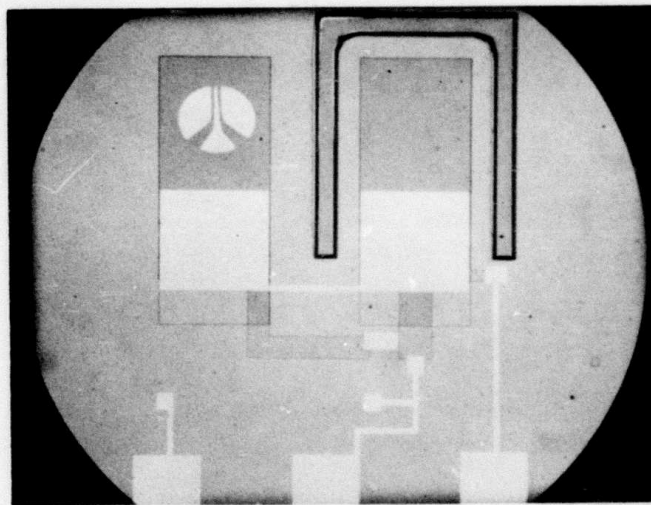
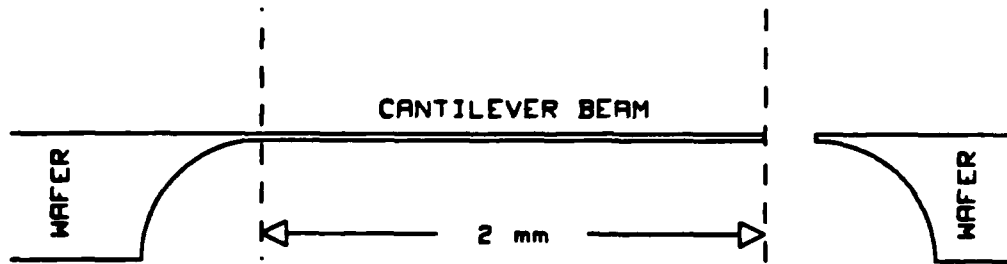
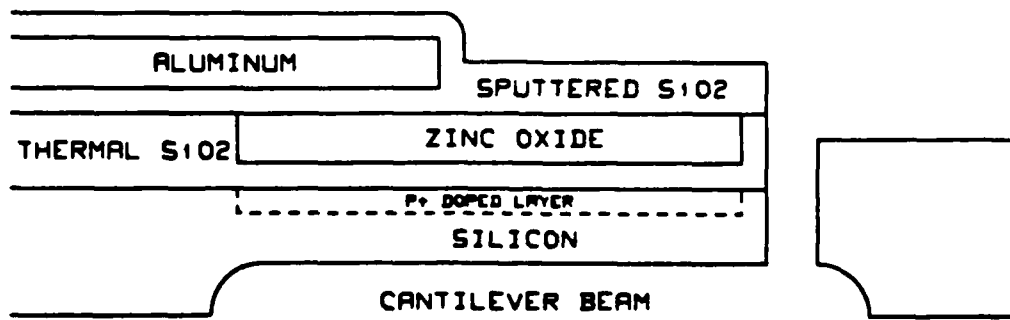


Fig. 11 A typical Si monolithic accelerometer sensor.

MRDC41082.16FR



(a)



(b)

Fig. 12 Detailed structure of a Si cantilever beam sensor: (a) cross section of beam; (b) scale-up cross section for clarity.

MRDC41082.16FR

electrostatic charge. The direction of this charge migration depends on the orientation of the crystallographic axes of the material, which must be controlled in the film.

In the Rockwell laboratory, ZnO is used as a piezoelectric film. ZnO has hexagonal crystal symmetry and pyroelectric sensitivity. The pyroelectric effect is one in which a change in temperature of the material causes the same sort of charge transfer as the piezoelectric capacitor. To eliminate sensitivity of the output bias of the monolithic accelerometer to temperature, a compensated capacitor is designed as part of sensor.

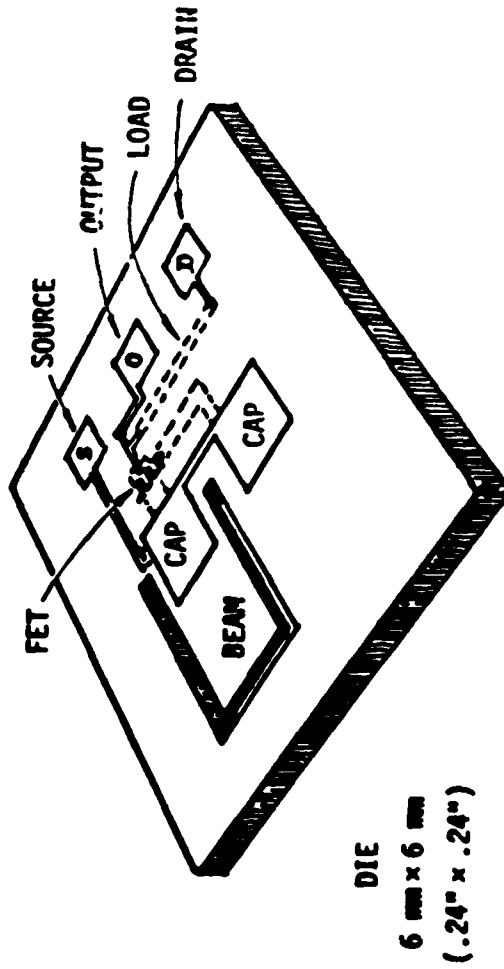
The piezoelectric capacitor is only a part of the IC that is designed into the monolithic accelerometer. The schematic circuit diagram in Fig. 13 shows two piezoelectric capacitors designed to cancel out the pyroelectric effect. (The piezoelectric capacitors are represented by capacitor symbols, with a shaded region on one electrode.) These piezoelectric capacitors are identically fabricated and connected in series, but back-to-back. In this configuration, the net output signal change due to a common temperature change is cancelled. However, if only one of these capacitors is on the cantilever beam, the signal due to the strain input (shown by the wiggly arrow) will appear at the PMOS gate. The PMOS gate isolates the capacitor circuit from ground, so that the stored charge (representing the input acceleration) does not decay over time. The degree of isolation was verified experimentally by straining the piezoelectric capacitor and by observing the PMOS output over a period of 24 h, then by releasing the strain and observing the PMOS output signal. The estimated decay time constant from this experiment was several days.

#### 5.4 Guidance System Simulation

The SAW resonator has a frequency stability of one part in  $10^{10}$ . This number is comparable to that of the bulk wave crystal oscillators. Since the frequency counting is gated in a short time (1 to 60 s), the value of  $10^{10}$  stability should be referred to as short-term frequency stability. The SAW

MRDC41082.16FR

Chip Layout



Circuit Schematic

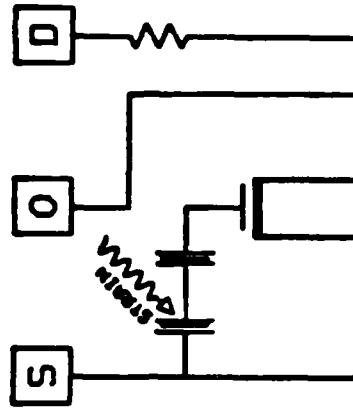


Fig. 13 Layout perspective of a cantilever SAM sensor with electrical equivalent circuit.

MRDC41082.16FR

resonator is a strain sensor; therefore, substrate material is contributing predominately to the device performance. Considering the temperature-stability requirement for some tactical missile applications, quartz substrate is chosen for the SAW resonator. Special orientation of quartz has temperature characteristics necessary to make temperature compensated SAW accelerometers.

Since the maximum allowable material strain for quartz is 200 ppm, for working at 10 Gs acceleration input, the device performs on scale factor of 20 ppm/G. Using these data, both bit quantization and frequency scale factor can be determined.

1. Bit quantization is defined as the smallest detectable velocity at the maximum acceleration input. Considering a center frequency of 376 MHz for the SAW resonator, the bit quantization of  $1.3 \times 10^{-3}$  m/s is achievable.
2. Frequency scale factor is defined, a count number of bits which is equivalent to the unit of the acceleration. Considering a center frequency of 376 MHz for the SAW resonator, a frequency scale factor of 769 Hz/m/s<sup>2</sup> has been achieved.

Shown in Fig. 14 is the actual count output of a SAW sensor when measured by a counter with a 1 s gate time. The difference frequency of 60 KHz has been subtracted, and only the deviation in the difference frequency ( $\pm 1$  Hz) is shown. Summing the counts results in the velocity count ( $\pm 10$  Hz) as a function of time shown. This curve represents the area under the acceleration-frequency curve. Performing another summation as a function of time results in the curve for displacement ( $\pm 4,000$  Hz). The integrated velocity error for the 1,000 s time period shown typically was less than 0.013 m/s, and the position error typically was less than 5.2 m. As expected, the integrated error is closely related to the integration time, and this is dependent on the actual mission time or time for which no other guidance data are available.



MRDC41082.16FR

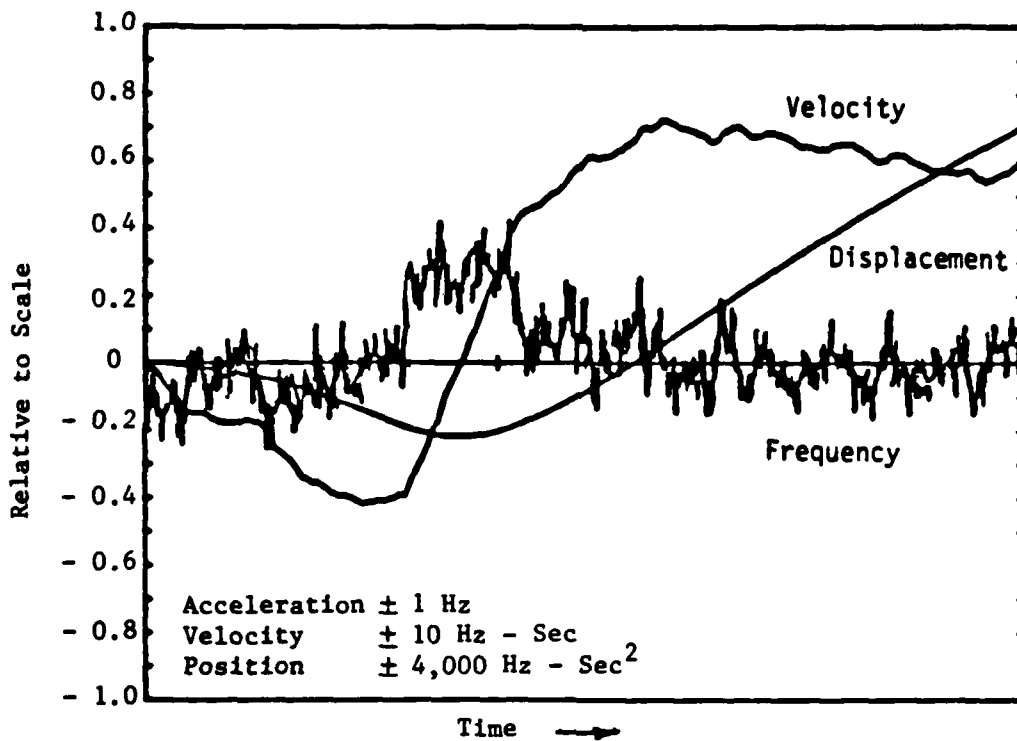


Fig. 14 Measured count output of a SAW dual crystal sensor vs time. Total time was approximately 18 min with a 2 s gate time. Also shown is the computed velocity from integrating once, as well as the displacement as a result of integrating the counter output twice.

## 6.0 RESULTS

### 6.1 Fabrication of SAW Resonators

The SAW resonator starting material is a Y-cut, single crystal quartz with an ultra-fine polish on one surface. Typically, the RMS surface roughness is less than 50Å. After the metal electrode pattern has been defined, the metal thickness is evaluated for the desired value, as well as a check of metal thickness uniformity. Uniformity of the deposited metal thickness is important to achieving resonators closely matched in frequency. An RF probing technique was used to measure the RF frequency prior to any other processing of the wafers. For example, the frequency sensitivity of Al electrode thickness was typically 1.67 KHz/Å at a nominal 350 MHz resonator. Maintaining a deposition uniformity of less than 5% is necessary to achieve devices with less than 200 ppm frequency variation.

To achieve high Q in SAW resonators, efficient surface wave reflection in the grating regions of the resonator must occur. This is done by photolithographically defining patterns on the wafers such that windows are opened in the reflecting grating regions of the resonator. The reflecting grating regions of the resonator are then ion-etched using a  $CF_4$  and oxygen mixture. The photoresist prevented etching of any of the transducer regions, and the Al in the grating regions acted as an etch mask, so that only the quartz between the grating was etched. The etching produces grooves between the reflector structure electrodes. The etching enhances the surface wave reflection at the grooves, and also lowers the resonant frequency of the gratings to coincide with the transducer frequency. This dispersion was accounted for in the original mask design with different periodicity between the gratings and the transducer. After plasma etching, the resist is removed and the resonators are pretested using an RF probe.

After pretesting, the wafers are diced and mounted. For the purpose of the aging testing program, the dicing format yields two resonators on the same chip. This structure is termed "dual crystal" and has been used exten-

sively in our testing of stability and aging. In the normal configuration, the dicing format has a single resonator per chip.

After dicing, the chips are mounted using a specially formulated, low outgassing, high temperature polyimide epoxy, which is vacuum-cured at 350°C. Following mounting, typically to a T0-5 to T0-8 header, the individual resonators were wire-bonded and a pretest of resonator characteristics was performed. Pretesting of the resonators yielded a device frequency, Q, and resistance before sealing.

A finished quartz wafer with a dual-crystal resonator is shown in Fig. 15. A T0-8 package with one device mounted is also shown in the same figure.

Sealing is done in a controlled glove box environment. The controls include an automatic pressure controller and a gaseous nitrogen system for removing all water vapor and oxygen from the glove box enclosure. A capacitance-discharge resistance weld is used to seal the flat package enclosure. The system has both input and output vacuum load locks. The input load lock chamber is a vacuum oven and a 24 h, presealed heating schedule. The output load lock is also a vacuum chamber for transporting the resonator package. After the vacuum bake cycle, the resonator is tested and the frequency is trimmed to the exact value. Now, the device is sealed under high vacuum.

## 6.2 Test Box Assembly

To have a fast turnaround for dynamic testing, a special test fixture that can accept a flat package was designed. This test fixture can be mounted directly on the shaker table, with four terminal outputs for signal processing. All terminals are available at OSM connectors which make the overall size of the box smaller. This test fixture has a volume of 10 cm<sup>3</sup> and a weight of less than 30 g.

The test box is a precise mechanical design with accurate orientation and flatness tolerance. The accelerometer is mounted such that the true device axis coincides with the test box design axis.

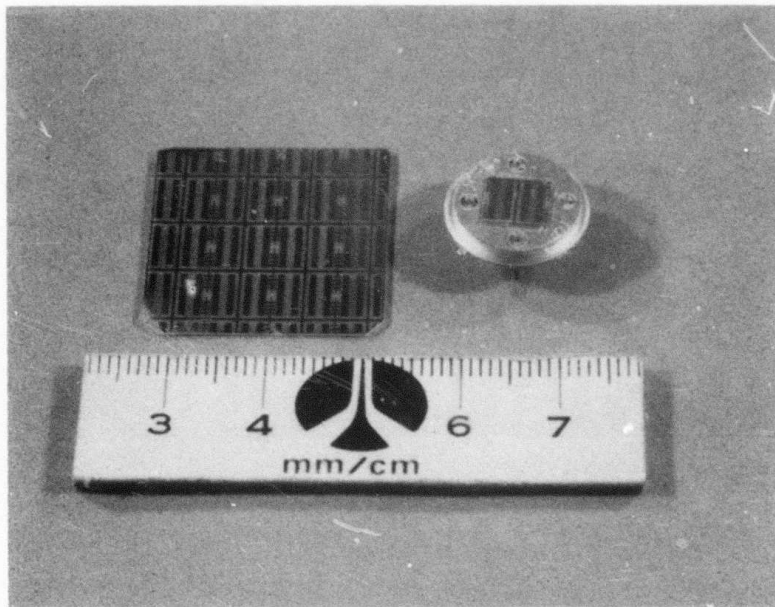


Fig. 15 A finished quartz substrate containing nine dual-crystal SAW resonators, including one mounted inside a TO-8 package.

MRDC41082.16FR

One important characteristic of the test box is the ability of multi-axis testing. To demonstrate the multi-axis experiment, we designed a special test box for vertically mounted and 45°-rotated Z-axis mounted accelerometers. To mount the accelerometer chip inside the flat package parallel to the test box, a special alignment technique is used to make the beam parallel to the package.

To analyze the data, a mathematical model for the operation of three orthogonally mounted accelerometer devices will be developed. The empirical data will be compared with the mathematical model to determine the degree of conformance of the empirical data with the theory. From the results of both the measurements and the mathematical model, scale-factor accuracy and linearity of three-axis accelerometers can be determined.

### 6.3 Dynamic Testing

For exact device characterization, a complete series of measurements must be made under varying acceleration conditions, so that a meaningful three-axis characterization and a correct algorithm, including all of the effects of cross-coupling, can be derived. When the acceleration is not in line with the design axis, the x, y and z components of acceleration must be taken into account in determining the response of the device.

By careful fixture design and mounting, these off-axis components can be evaluated in the single device through a series of accelerometer tests with variable input axes to the accelerometer device. The nature and magnitude of the cross-coupling, three-axis measurements on a single device will first be carefully evaluated to better understand single device characteristics.

Based on the results of this kind of test, three accelerometers will be mounted in the three-axis planes of a test box and simultaneous data will be taken. This fixture will then be evaluated at various acceleration angles and magnitudes while maintaining separate data channels for each device. Thus, an empirical assessment of the three-axis performance of the monolithic accelerometer can be accomplished. The multi-axis measurement is a powerful

MRDC41082.16FR

technique for characterizing the cross-axis error presented in most navigation systems.

Figure 16 shows a typical output response of the accelerometer at 5 Gs and 100 Hz, which is the result of a single axis measurement. For this measurement, the spectrum analyzer was set to a 36.3 Hz bandwidth and the device shows a scale factor of 7 mV/g.

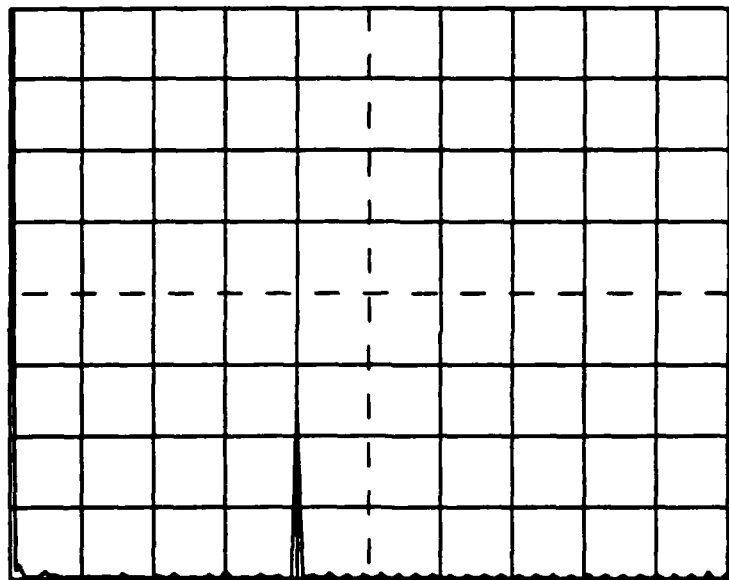
The results of typical cross-axis data are shown in Fig. 17. The response shown in the figure is when the accelerometer is mounted vertically. In this case, the cross-axis signal is visible at 200 Hz and 5 G. For comparison, the same device was mounted horizontally with designed axis, and the data were taken in the identical test parameter. The results are shown in Fig. 18.





MRDC41082.16FR

CH A: 400  $\mu$ V FS 50.0  $\mu$ V/DIV

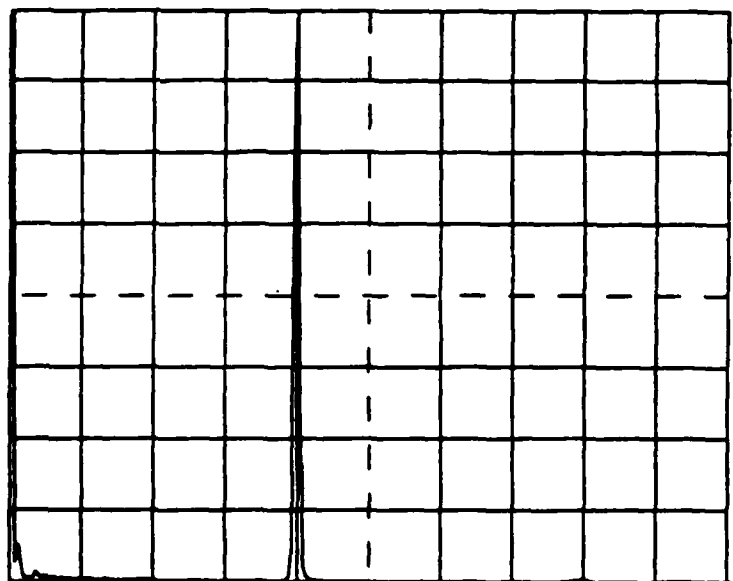


\ 0 Hz 5 KHz /  
PEAK: 153  
EP-105 M-AXES DATA TIC

Fig. 17 A typical cross-axis response of a SAW accelerometer sensor at 2000 Hz.

MRDC41082.16FR

CH A: 400  $\mu$ V FS 50.0  $\mu$ V/DIV



\ 0 Hz 5 KHz /  
PEAK: 165 BW: 30.0 Hz  
EP-105 M-AXES DATA H1C

Fig. 18 A typical true-axis response of a SAW accelerometer sensor at 2000 Hz.

## 7.0 FUTURE PLANS

The results of this program established a complete SAW sensor fabricated on a quartz substrate. The device showed high short-term stability and excellent frequency scale factor. During the term of this work, we were not able to make a prototype accelerometer with the proposed requirement. The following tasks should be accomplished for the required accelerometer.

1. For the highly sensitive accelerometer, the quartz cantilever beam should have a hammer-head shape. Our study showed that a two-dimensional shape is practical, but is not adequate to produce enough sensitivity. Therefore, a three-dimensional quartz cantilever beam should be studied.
2. For the requirement in frequency stability, device packaging should be investigated. This study has already started under this program, but it is necessary to continue the research for a better solution.
3. A complimentary technique using a Si-based accelerometer should be studied for the purpose of fast reaction time devices. This phase was also initiated under the present contract, but needs more investigation.

MRDC41082.16FR

## 8.0 REFERENCES

1. M.E. Motamedi and A.P. Andrews, "Monolithic Accelerometer," Final Report, Contract No. DASG60-83-C-0101, June 1985.
2. W.E. Rosvold and M.L. Stephens, "Cantilever Accelerometer," AFAL-TR-77-152, WPAFB, OH, 1977.
3. M.E. Motamedi, "Passivation on High-Q Acoustic Strain Sensors for Accelerometer," Final Technical Report, Contract No. F49620-82-C-0012, November 1984.

## APPENDIX A: RESEARCH FACILITIES

Facilities offer 10K sq ft of class 10,000, with class 100 working areas for wafer processing and 5K class 30,000 area for assembly process line. The areas involved are secured for classified material. Facility capabilities include MIL-M38510 compliance, MIL-Q-9858 quality system, MIL-STD-883 screening and burn-in, and MIL-C:45662 traceability and calibration. The assembly process line has a packaging capability of 5,000 per week for a variety of different package types such as ceramic hermetic, dips, flatpacks, LLCC and LCC. A number of aligners are currently in use. The Perkin Elmer projection aligners, GCA-MANN 4800 DSW and Cannon 4X projection aligner are among these. Also, a new Censor SRA-100 automatic step-and-repeat projection aligner (Fig. A.1) has been purchased recently and is now in use at the MRDC Thousand Oaks facility. A Jade step-and-repeat projection aligner is now being used exclusively for DSW and mask processing of SAW devices (Fig. A.2). For high resolution lithography, a Cambridge MF-6 electron beam system is being used at the same facility. The pattern generator tapes for mask production are made using the Calma GDS11 CAD system. Recently, a second color terminal which greatly enhances the turnaround time has been added to the system.

A HP8510 network analyzer is used in conjunction with a HP9836 computer for automated measurements involving SAW devices (Fig. A.3). The HP8510 is the most advanced network analyzer available at the present time. The system is equipped with the time-domain measurement and phase-locked system.

Test systems such as the Tektronix 3260 (wafer probe, package test, environmental characterization), Accutest 7900 (50 MHz, 60 dual I/O channels, temperature testing) are being used routinely for testing and characterization at the center. A CVD reactor for  $\text{Si}_3\text{N}_4$  and dry etching of Si and oxide (Fig. A.4) and an RF sputtering system for deposition of ZnO films (Fig. A.5) are also being used in SAW processing.

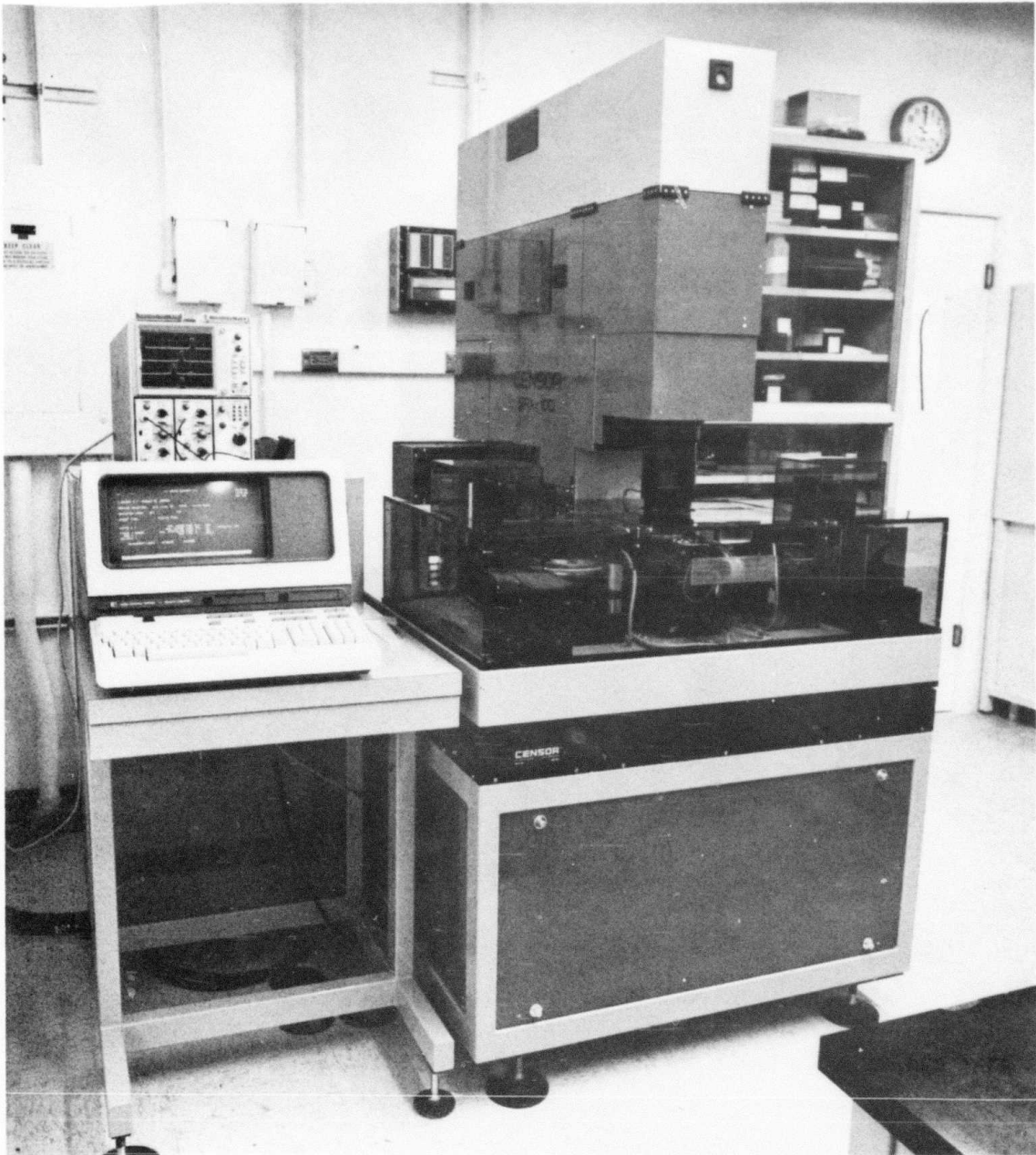


Fig. A.1 Censor SRA-100 automatic step-and-repeat mask aligner and exposure system.

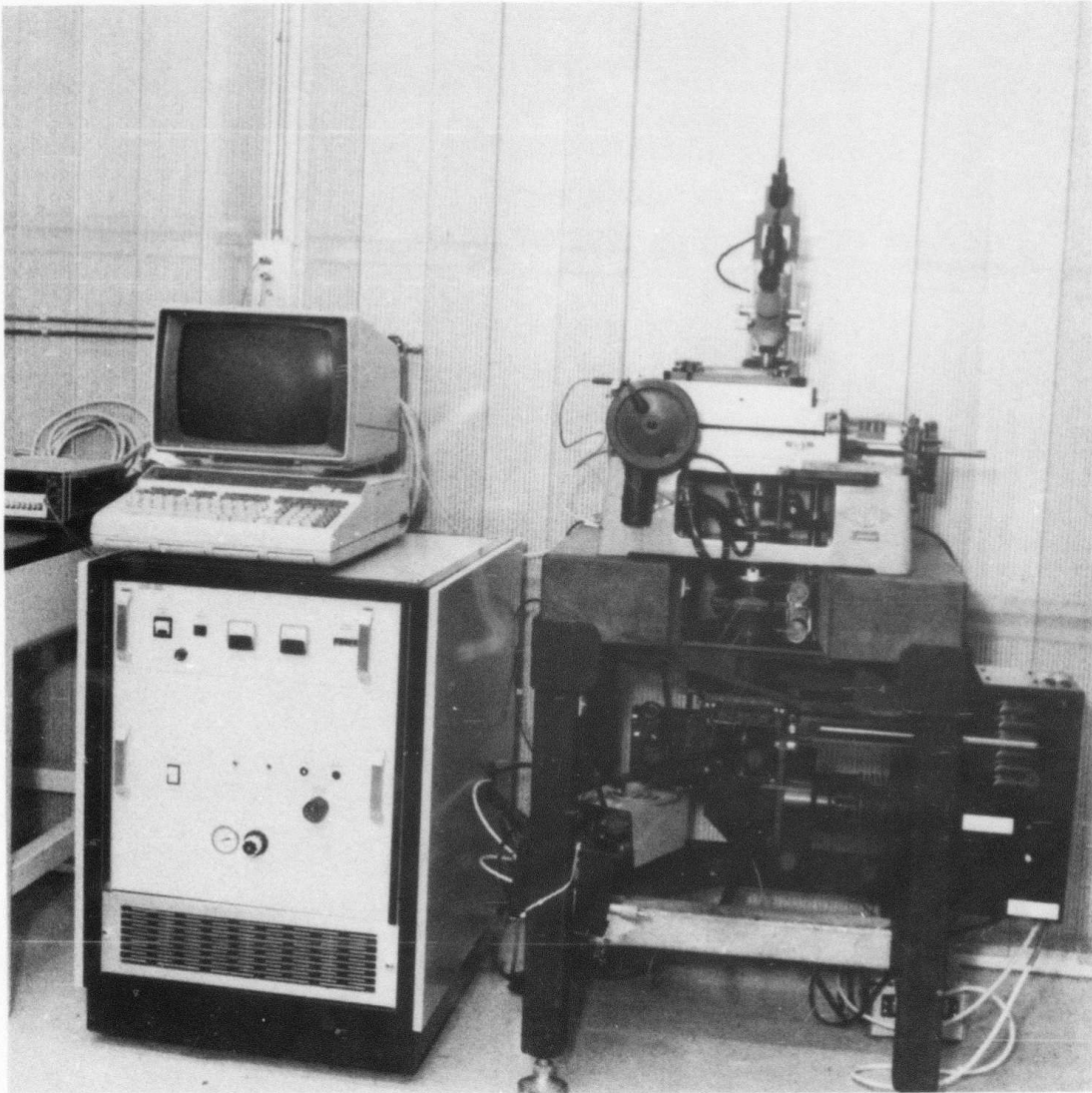


Fig. A.2 JADE step-and-repeat projection aligner for DSW and mask processing.



Fig. A.3 HP-8510 network analyzer with HP9836 controller.

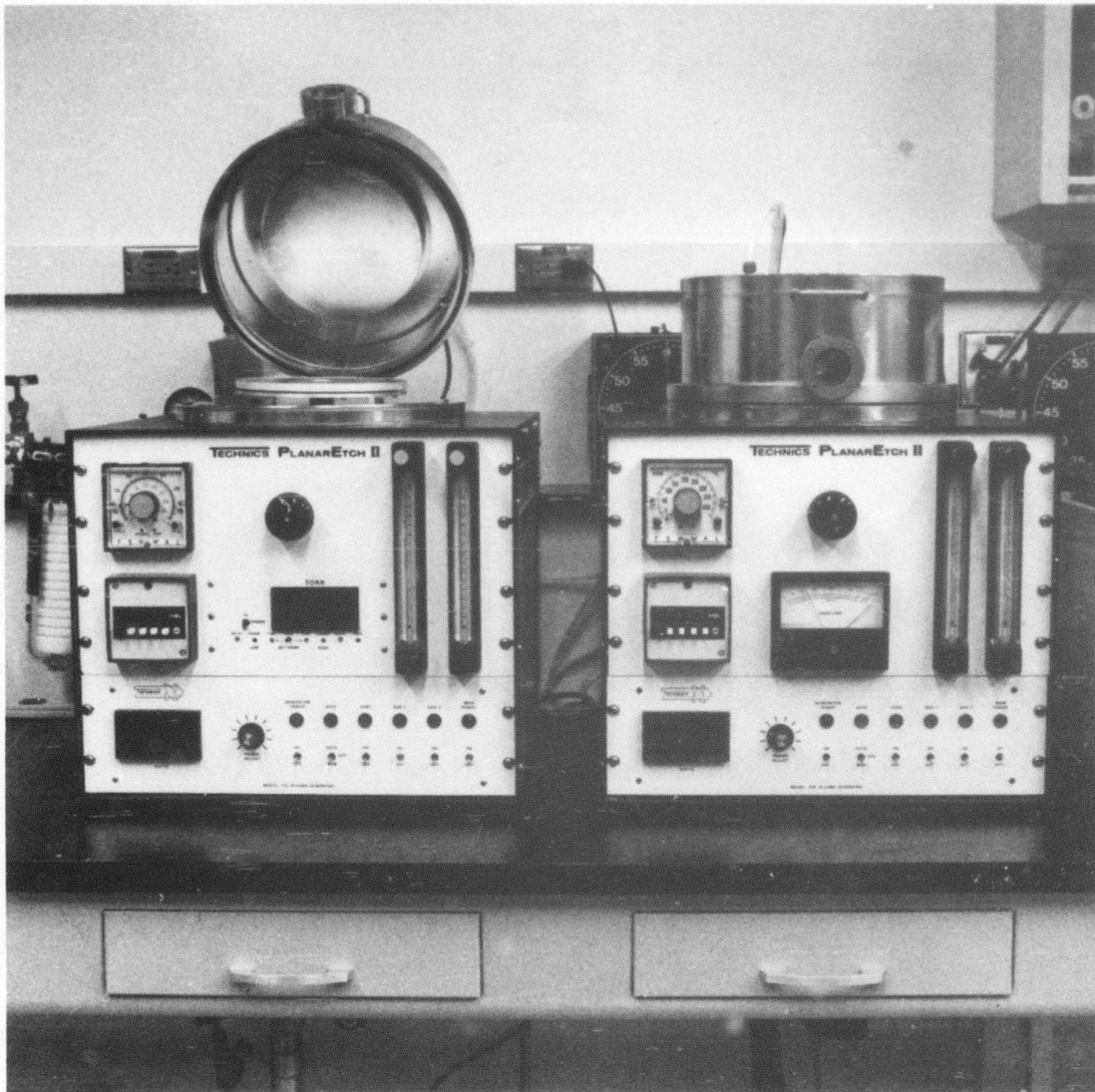


Fig. A.4 CVD reactors.



Fig. A.5 RF sputtering system.

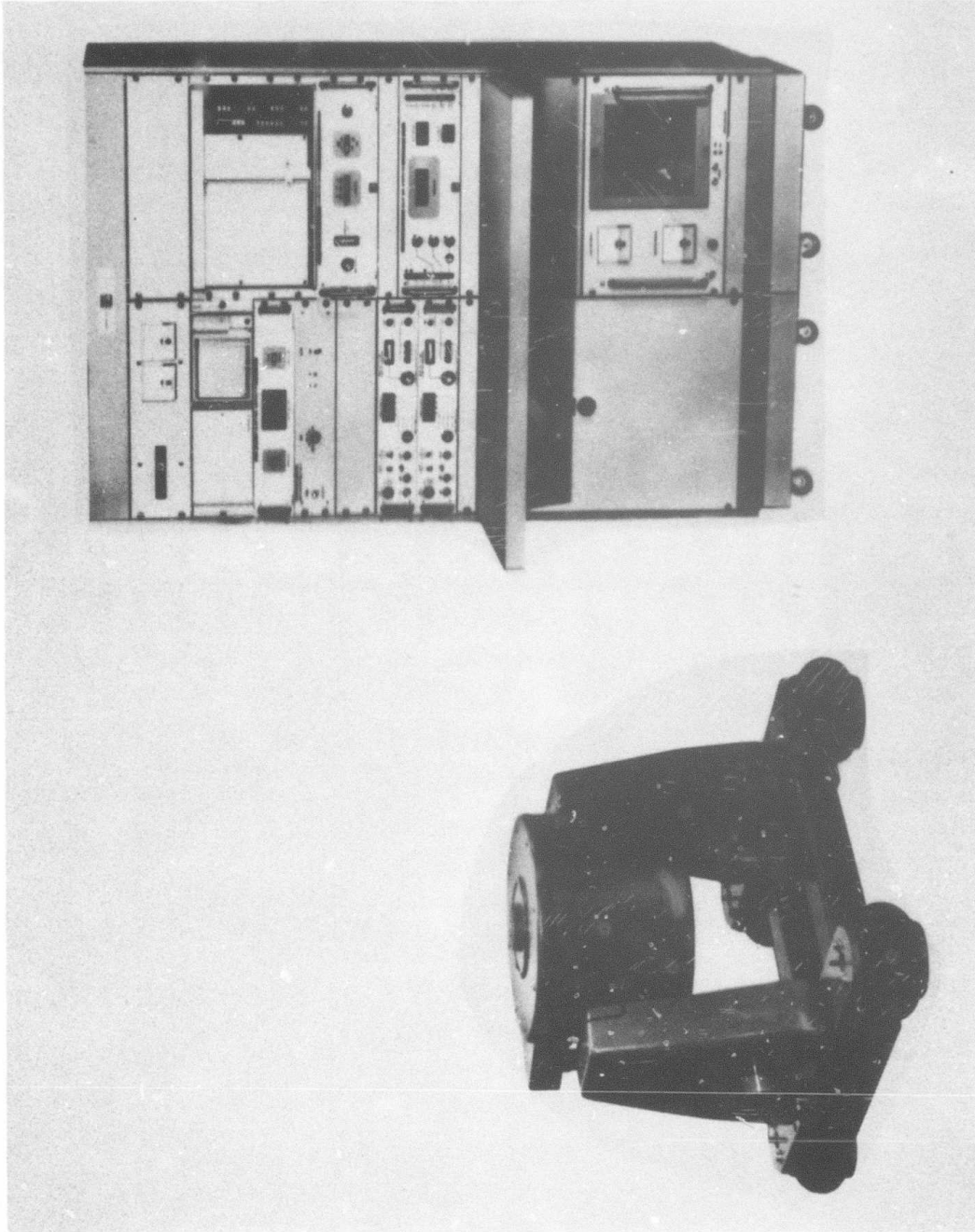
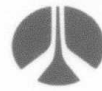


Fig. A.6 Unholtz-Dickie Model 351 dynamic shaker.